INTERNATIONAL JOURNAL OF HYDROGEN ENERGY ▮ (▮▮▮▮) ▮▮▮–▮▮▮

Available at www.sciencedirect.com

ScienceDirect

journal homepage: www.elsevier.com/locate/ijhydene

Thermal stress analysis of the planar SOFC bonded compliant seal design

*K.S. Weil**, *B.J. Koeppel*

Pacific Northwest National Laboratory, P.O. Box 999, Richland, WA 99352, USA

ARTICLE INFO

Article history:
Received 4 June 2007
Received in revised form
6 November 2007
Accepted 7 November 2007

Keywords:
Planar solid oxide fuel cell
Bonded compliant seal
Finite element analysis
Thermal stress

ABSTRACT

A new materials joining approach known as the bonded compliant seal (BCS) has recently been developed for hermetically sealing the cell and window frame components in planar solid oxide fuel cell stacks. At the heart of the BCS is a thin deformable metal foil that is designed to decouple the effects of differential thermal expansion between the two components and thereby mitigate the generation of potentially destructive thermal stresses in the stack. While preliminary viability of the BCS design has been demonstrated in small-scale rotationally symmetric test specimens, issues concerning the scale-up of this seal to a size and shape that is prototypic of full-size stacks are addressed here. Finite element analysis was undertaken to investigate the magnitudes of thermally induced stress, strain, and part deflection in the cell, seal, and window frame components under uniform heating and cooling conditions. From the point of stress mitigation, particularly in the brittle ceramic cell, the initial BCS design appears to function quite well by accommodating the mismatch thermal strains as elastic and plastic strain within the sealing foil. However, the model predicts that some bowing will take place within the cell. While the amount of bowing is likely manageable through proper design of the adjacent interconnects, it is believed that a substantial portion of the predicted bow can be eliminated via minor adjustments to the various seal parameters.

Published by Elsevier Ltd. on behalf of International Association for Hydrogen Energy.

1. Introduction

Planar solid oxide fuel cells (pSOFCs) are compact devices that convert chemical energy into electrical energy via an oxygen ion gradient that develops across a thin ceramic electrolyte. Because of this, hermeticity across this solid membrane is paramount. The presence of leaks, either due to flaws that originate during stack manufacture or that form because of component degradation during stack operation, lead to reduced system performance, lower power generation efficiency, and poor fuel utilization [1,2]. In addition they can cause local hot spots or worse, widespread deflagration within the stack, both of which induce accelerated degradation in the device [2]. In a planar stack design, this means that the electrolyte layer must be dense and connected to the rest of the device with a high temperature, gas-tight seal. One of the fundamental challenges in fabricating pSOFCs is how to effectively join the thin electrochemically active ceramic cell to the metallic body of the device and thereby create a rugged, hermetic, and chemically stable seal. Typical conditions under which these devices are expected to operate and to which the accompanying seals will be exposed are: (1) an average operating temperature of 750 °C; (2) continuous exposure to an oxidizing atmosphere on the cathode side and a wet reducing gas on the anode side; and (3) an anticipated device lifetime of 10,000+ hours.

Recent reviews by Fergus [3] and Weil [4] describe in detail the various processes and materials used in sealing planar

*Corresponding author. Tel.: +1 509 375 6796; fax: +1 509 375 4448.
E-mail address: Scott.Weil@pnl.gov (K.S. Weil).
0360-3199/$ - see front matter Published by Elsevier Ltd. on behalf of International Association for Hydrogen Energy.
doi:10.1016/j.ijhydene.2007.11.008

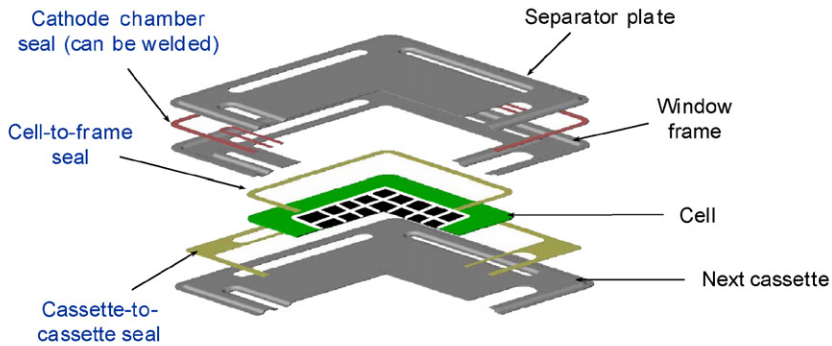

Fig. 1 – A schematic of the cell-to-frame pSOFC design.

SOFC devices. Essentially there are two types of cell-to-frame seals that designers currently employ in the common window frame pSOFC stack design: (1) rigid bonded glass seals and (2) compressive gasket seals. As shown in Fig. 1, the window frame design is built around a metallic window frame, which along with a metal separator plate and ceramic cell, form the repeat unit in the stack. The frame affords an easy and reliable means of gas manifolding within the stack and its geometry establishes a uniform gap for air flow across the cathode. Typically two seals are employed in this design, one between the cell and window frame/separator plate assembly to form a cassette repeat unit and a second seal between each cassette in the stack. Of the two, the window frame seal presents the greater engineering challenge because it is a joint between two distinctly different materials; i.e. a metallic frame and a ceramic membrane.

The advantages and disadvantages of the rigid bonded and compressive seals have been previously discussed in Refs. [3,4]. In brief, compressive seals offer excellent material compliance and therefore the capacity to accomodate large mismatch strains between components that display significantly different coefficients of thermal expansion; e.g. the type seen in the cell and frame materials. However, rigid bonded seal designs eliminate the need for a load frame, which is required in gasket-type seals. This is particularly advantageous in mobile or transportation applications. In addition, rigid bonded seals are less prone to leakage over long-term use. However, they do not afford the same degree of design flexibility that compressive seals offer. As a result, a third sealing option known as the bonded compliant seal or BCS is being developed that conceptually incorporates the advantages of both rigid and compressive sealing.

Composed of a thin, deformable metal foil that is bonded to the adjacent metal and ceramic components, the BCS is expected to display excellent hermeticity and high mechanical integrity under thermal cycling and mechanical vibration, while mitigating thermal mismatch stresses in the ceramic cell by "trapping" much of it as elastic or plastic strain within the sealing foil. One of the primary advantages that this type of seal offers is that a much wider range of alloy compositions can be considered for use in the pSOFC interconnect. At present, the candidate list is restricted only to those that offer good CTE matching with the ceramic cell, namely the chromia scale-forming ferritic stainless steels. Unfortunately, these alloys generally display poorer mechanical, oxidation, and through-scale electrical properties than their nickel-based counterparts [5] as well as contribute to long-term degradation in stack performance via chromia vaporization and poisoning [6].

An initial proof-of-concept demonstration showed that small-scale BCS joints are hermetic and display good strength in both the as-joined and thermally cycled conditions (tested at 75 °C/min over a temperature range of 25–750 °C) [7]. The specimens used in these studies employed a stamped 50 μm thick fecralloy foil brazed to a nickel-based superalloy washer and a 25 mm diameter × 600 mm thick NiO–YSZ anode/YSZ electrolyte bilayer disc. That is, the specimens were small in size and rotationally symmetric. A recent comparative analysis [8] performed using finite element (FE) computations indicated that the BCS potentially offers substantial advantages over glass–ceramic and brazed seals [9] with respect to mitigation of thermal stresses, particularly in the ceramic cell. Based on these results, the present study was undertaken with goal of determining the viability of the BCS design in a shape and size that is more prototypic of an actual stack. To do this, FE analysis was employed to model and compare the magnitude of mismatch stresses/strains that arise in each of the seal components during a uniform stack heating/cooling sequence.

2. Modeling parameters

The ANSYS 8.0 software suite was used to carry out three-dimensional (3-D) FE analyses of a full-scale, square-shaped BCS design. Depicted in Figs. 2(a) and (b) are cross sections of the modeled seal. The individual components in the seal are labeled in Fig. 2(a), while Fig. 2(b) shows how the FE mesh was configured within each component. Because the planar geometry of the ceramic cell displays fourfold symmetry, a one-quarter model was employed to reduce the computation time. Like the specimens tested in Ref. [7], the model seal consists of a cell brazed to a stamped S-shaped fecralloy foil using a silver-based ceramic-to-metal air braze filler metal, Ag-4 mol% CuO [9]. On the opposite side, the fecralloy foil is brazed to a Haynes 214 window frame using a conventional high-temperature braze filler metal, AMS 4777 (7.0 wt% Cr, 3.0 wt% Fe, 4.5 wt% Si, 0.06 wt% C, 3.2 wt% B, balance Ni).

Please cite this article as: Weil KS, Koeppel BJ. Thermal stress analysis of the planar SOFC bonded compliant seal design. Int J Hydrogen Energy (2007), doi:10.1016/j.ijhydene.2007.11.008

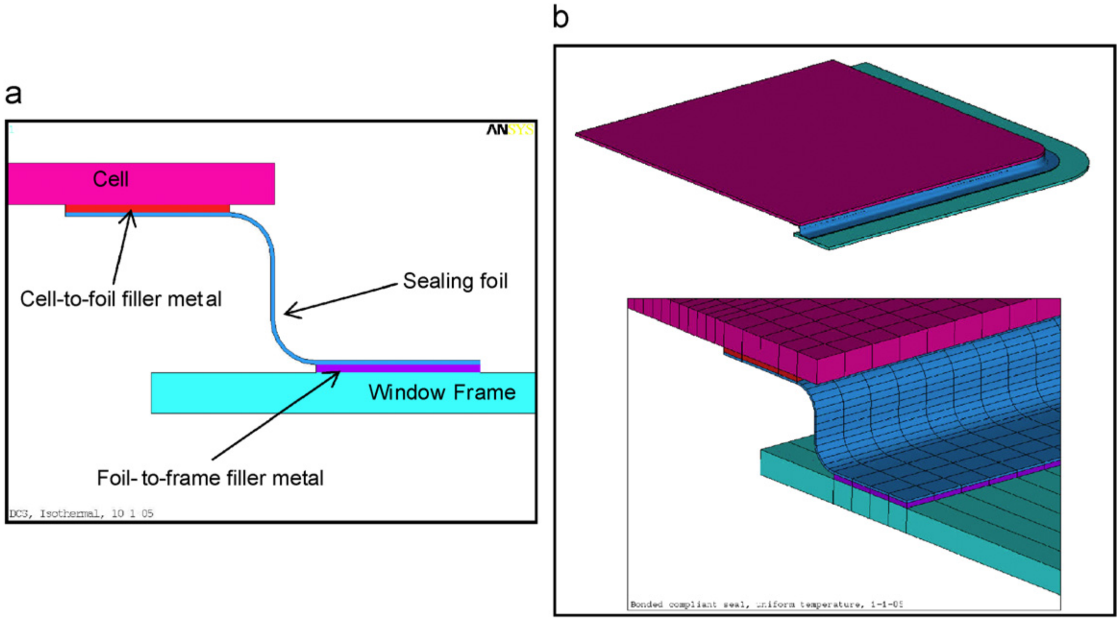

Fig. 2 – (a) A schematic of the BCS design in cross section. (b) A one-quarter symmetry model of the BCS design.

Haynes 214 was chosen for this analysis because it is representative of the type of alumina scale-forming alloy that is of particular interest in an SOFC stack design [5]. In addition, the CTE of this material is nearly 50% greater than that of the anode supported cell (15.7 vs. 10.6 μm/m K); i.e. this type of materials set constitutes a significant dissimilar materials joining challenge. The ceramic cell was modeled as a monolith measuring 500 μm thick × 120 mm square with 10 mm radii corners, which approximates the size of cells used in several actual stack designs [10,11]. In reality, the cells employed in planar stacks are typically anode supported (450−570 μm thick) with a thin electrolyte layer (5−8 μm thick) and a thin cathode layer on top (15−20 μm thick). However, with respect to establishing the mechanical properties and FE mesh for this component in the present analysis, a simplifying approximation was employed in which the cell was treated computationally as a single material; i.e. the Ni–YSZ anode material. Listed in Table 1 are the dimensions and compositions of the seal components that were used as inputs to the FE model.

Table 1 – Component dimensions and materials database properties employed in modeling

Component	Thickness (μm)	Material
Cell	600	Ni–YSZ/YSZ
Cell-to-foil braze	100	Ag-4 mol% CuO
Sealing foil	50	FeCrAlY
Foil-to-frame braze	100	BNi-2 Braze
Frame	500	Haynes 214

The ANSYS code is convenient because it allows the input of user defined constitutive models as well as control routines to obtain a convergent solution. Except for the cell, the mechanical properties of each component were treated using a bilinear elastic–plastic constitutive model with kinematic hardening. That is, the elastic modulus was used to describe stress–strain behavior up to the point of yielding, beyond which an average value of hardening modulus provided the mechanical characteristics in the plastic regime. In this way, a set of temperature dependent stress–strain equations could be developed for each constituent material. The data used in these equations were obtained from the alloy manufacturers and/or reference handbooks [12–14]. The corresponding stress–strain curves are shown in Figs. 3(a)–(d). In the case of the anode or cell material, elastic property data generated from ultrasonic pulse-echo testing of the reduced Ni–YSZ cermet at various temperatures was employed [15]. A CTE curve for each material was also obtained from either reported manufacturer's data or through in-house testing [12–15]. In this initial simplified analysis, material creep was not considered.

Eight-noded brick elements with three translational degrees of freedom were employed in constructing the FE meshes for each component in the seal. In general, the model's accuracy increases with more nodes and therefore greater mesh refinement [16]. However, there is a point of diminishing returns beyond which further refinement offers little improvement in accuracy. At the same time, the mesh density is restricted by computational time limits that are considered reasonable. The current mesh configuration was chosen as an effective compromise in this preliminary parametric study. A fine mesh was used in the regions of interest, e.g., corners, while a coarser mesh was developed to capture the overall structural response in the rest of the model. An enhanced strain formulation was used with the single layered elements to adequately capture the bending response. A uniform temperature load condition was applied to investigate the location and magnitude of thermally

Please cite this article as: Weil KS, Koeppel BJ. Thermal stress analysis of the planar SOFC bonded compliant seal design. Int J Hydrogen Energy (2007), doi:10.1016/j.ijhydene.2007.11.008

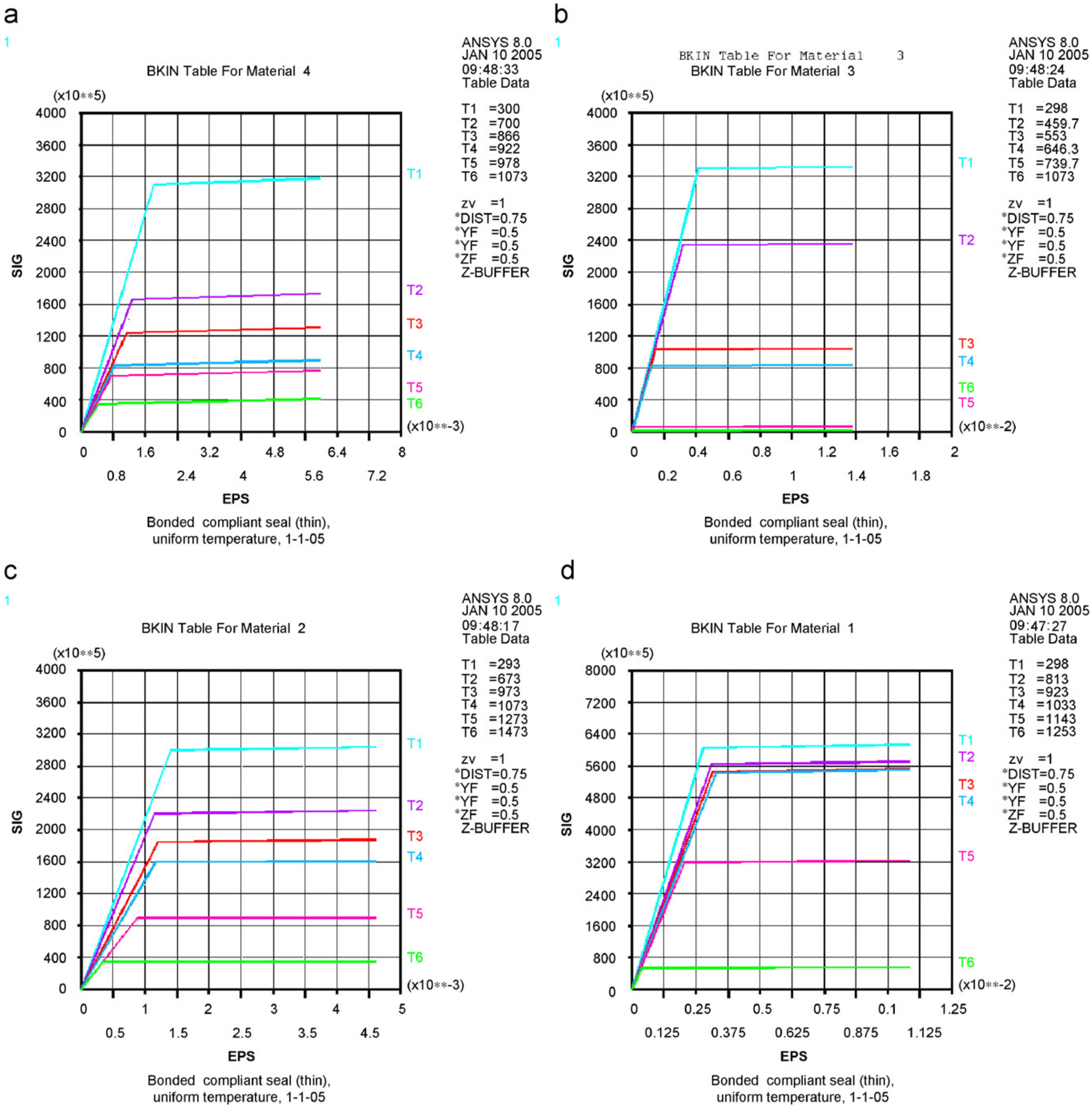

Fig. 3 – Examples of the bilinear stress–strain curves employed in FE analysis: (a) Ag–CuO filler metal, (b) fecralloy, (c) AMS 4777 filler metal, and (d) Haynes 214.

generated mismatch stresses and out-of-plane strains. That is, in each iteration as the temperature was increased or decreased to account for a given part of the thermal cycle, all of the components in whole were assigned the same temperature. Alternatively, it could be considered that the entire structure is heated or cooled at a very slow rate, thereby establishing an isothermal condition. The starting temperature in the analysis was that typically used to conduct the final cell-to-foil joining sequence, 1273 K (1000 °C), which effectively defines a stress-free state for the structure. After which the structure was cooled to an assumed operating temperature of 1073 K (800 °C), then subsequently cooled to room temperature (298 K, 20 °C), re-heated to 1073 K, and re-cooled to 298 K, as shown in Fig. 4, to examine the effects of a first and second thermal cycle on the generation of mismatch stresses in the various seal components. The boundary conditions used in the analysis were: (1) the application of symmetry conditions for a one-quarter model to minimize computational time and data storage space and (2) the out-of-plane displacements for the bottom of the window frame were constrained to zero, permitting only 2-D in-plane deformations. However, out-of-plane component deflections were allowed throughout the rest of the model.

Please cite this article as: Weil KS, Koeppel BJ. Thermal stress analysis of the planar SOFC bonded compliant seal design. Int J Hydrogen Energy (2007), doi:10.1016/j.ijhydene.2007.11.008

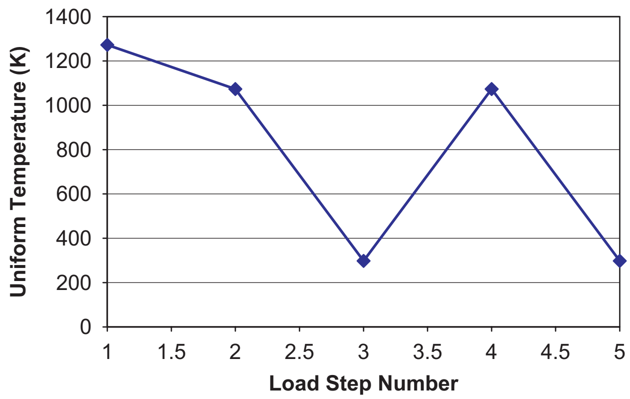

Fig. 4 – A plot of the thermal cycle incorporated in the present FE analysis model.

3. Results and discussion

3.1. *Stress and strain distribution as a function of temperature*

Shown, respectively, in Figs. 5 and 6 are the stress and strain distributions predicted in the BCS structure when it is cooled from a stress-free state at 1273 K to an operating temperature of 1073 K. The maximum principal stress and elastic strain are shown for the ceramic anode layer, while von Mises stress and equivalent total strain are shown for the remaining ductile materials. In the cell, cell-to-foil braze filler metal, and foil, the highest levels of stress arise in the corners of each component. Note that the stresses in the silver-based cell-to-foil braze are low due to its comparatively low yield strength at this temperature. This results in local strains above 0.5%, i.e. plastic yielding, as seen in Fig. 6(b). The deformation observed in this layer accommodates to a large degree the thermal mismatch between the braze layer and the adjacent cell and sealing foil components, keeping stresses in the latter two quite low. Because the thermal contraction of the silver-based filler metal is significantly greater than that of the cell, narrow regions of compressive stress arise in both the corner and along the edges of the cell where the two components contact. Low stresses are also observed in the AMS 4777 braze layer and adjoining window frame component and the stress/strain distributions in each tend to be more uniformly spread over the sealing region.

Shown, respectively, in Figs. 7 and 8 are the predicted principal stress and strain distributions in each BCS component when the entire structure is uniformly cooled to room temperature. Again there appears to be a some stress concentration in the corners of the components, similar to what Lin et al. reported in rectangular-shaped glass-sealed pSOFC stacks [17], but the ratio of $\sigma_{max}/\sigma_{min}$ in each case generally tends to be smaller than that predicted for cooling from 1273 to 1073 K. In addition, while the thermally induced mismatch stresses in the cell and window frame components continue to increase upon cooling through the operating temperature to room temperature, their magnitudes remain well below those required, respectively, for fracture or yielding (~50% of $\sigma_{avg,fracture}$ in the case of the cell and ~10% of σ_{yield} for the Haynes 214 window frame material) [15,12]. There are two reasons for this: (1) the silver cell-to-foil braze material undergoes nearly uniform plastic deformation and (2) the sealing foil plastically deforms along the vertical crease (between the upper and lower sealing surfaces) and elastically deforms by bending out of plane.

Summarized in Table 2 are the largest principal stresses and strains in the ceramic cell and the maximum equivalent stresses and strains in each elastic–plastic component upon cooling to 1073 K and to room temperature. Note that at room temperature, the largest stresses and strains in the overall seal structure are localized within the deformable foil and the air braze. That is, the seal appears to function as desired, preventing excessive thermally induced stresses in the cell and window frame by concentrating the mismatch thermal strain as elastic and plastic strain within the thin sealing foil and the adjacent soft silver filler metal. The resulting effect is equivalent to other compliant structures that serve a similar purpose; for example, in bonded semiconductor chips, where compliant lead structures have been developed to overcome solder joint failure due to thermal fatigue and in nuclear reactor where the accommodation of swelling due to irradiation is required for successful operation [18,19].

Upon re-heating from room temperature back to operating temperature, stresses in each component correspondingly drop, as seen in Figs. 9(a)–(e). It should be noted that relative to the prior cycle at 1073 K (Figs. 5 and 6), the levels of stress experienced in the second thermal cycle are lower in each component and that there is greater uniformity in their spatial distribution. The same is true when the structure is cooled for a second time to room temperature, although the differences between the 1st and 2nd cycles at this temperature are smaller, as seen in Figs. 10(a)–(e). The maximum stresses and strains predicted in the second thermal cycle are listed in Table 3. Comparison of these values with those in Table 2 confirms that the thermally induced stresses and strains predicted in a second thermal cycle are lower than those calculated for the initial cooling sequence. Again, this is due primarily to plastic deformation in the cell-to-foil braze material and elastic deflection in the sealing foil. As will be discussed, the foil tends to deflect out of plane primarily by simple rotation of the upper sealing surface relative to the lower one along the long edges of the foil and by a more complex cup-shaped bending motion around each corner.

In the BCS design, there are a number of parameters that potentially can be modified or adjusted to further reduce stress in the various sealing components (specifically the brittle cell) including: the thickness, modulus (i.e. composition), and cross-sectional shape of the sealing foil; the size of the corner radii in the cell and other components; the thickness, modulus, and coefficient of thermal expansion of the cell-to-foil filler metal; the areas of contact at the cell-to-foil filler metal/cell and filler metal/foil junctions; and the thickness and modulus of the window frame. While the resulting effects are still being investigated in a design parameter sensitivity analysis, recent calculations made with models incorporating modest changes in foil thickness (±10%) illustrate how the design can be further tailored. Reported in Tables 4 and 5 are results from the same type of FE analysis as above for BCS designs employing a sealing foil

Please cite this article as: Weil KS, Koeppel BJ. Thermal stress analysis of the planar SOFC bonded compliant seal design. Int J Hydrogen Energy (2007), doi:10.1016/j.ijhydene.2007.11.008

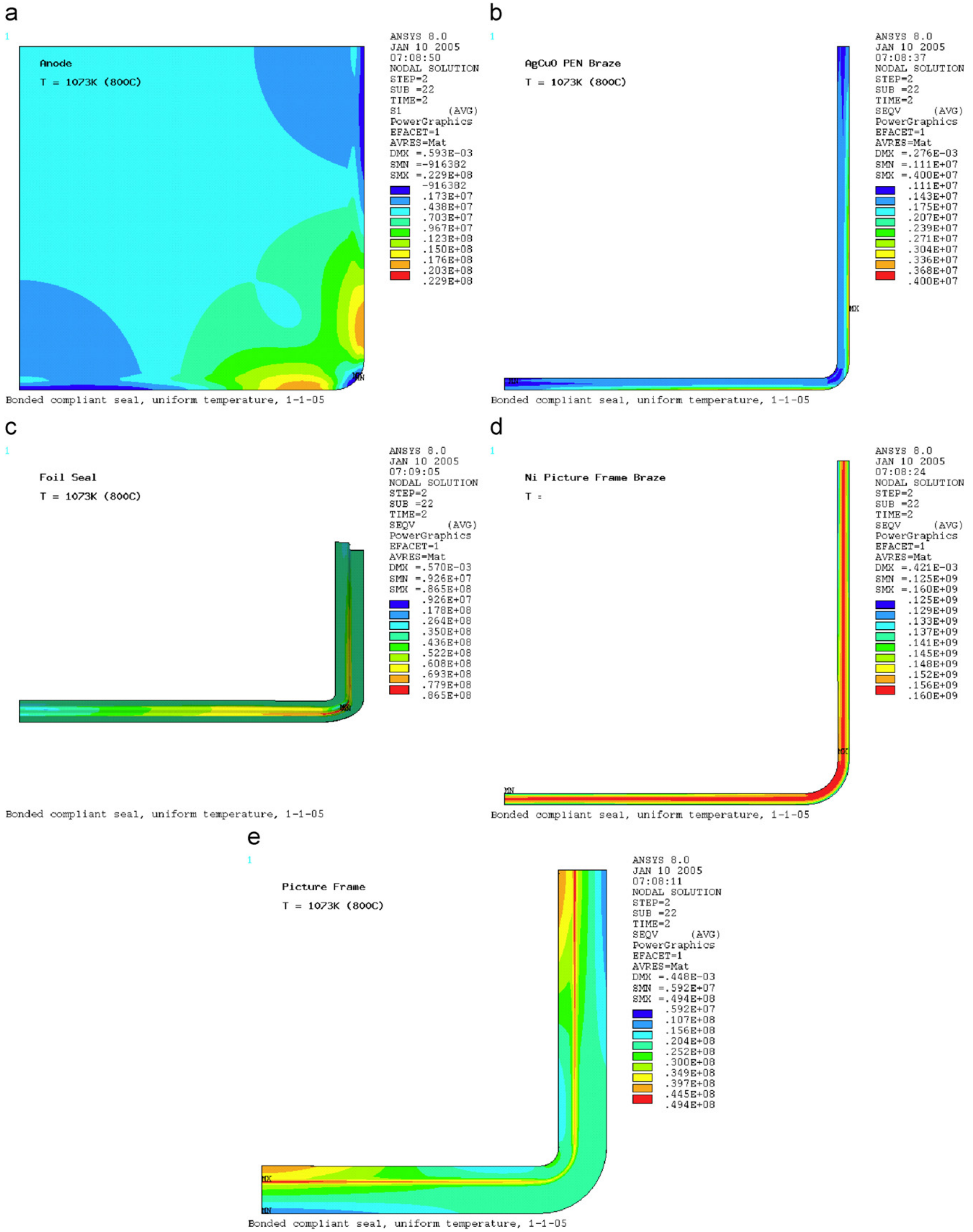

Fig. 5 – Stresses predicting upon cooling from a stress-free state at 1273 K to an operating temperature of 1073 K for: (a) the cell, (b) the cell-to-foil filler metal, (c) the sealing foil, (d) the foil-to-frame filler metal, and (e) the window frame. Note that the values corresponding to the scale bars listed on the right-hand side of each figure have units of Pa.

Please cite this article as: Weil KS, Koeppel BJ. Thermal stress analysis of the planar SOFC bonded compliant seal design. Int J Hydrogen Energy (2007), doi:10.1016/j.ijhydene.2007.11.008

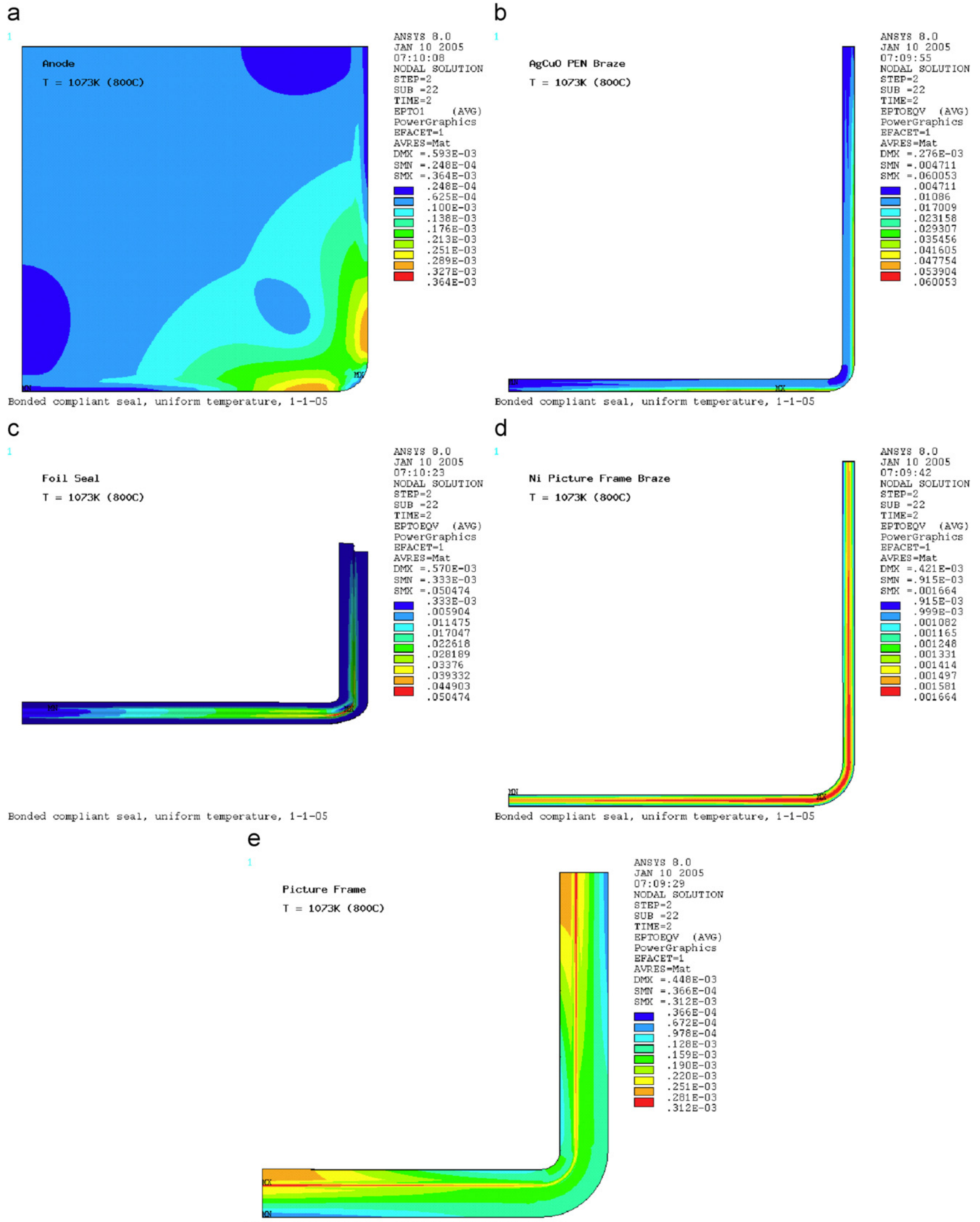

Fig. 6 – Strains predicting upon cooling from a stress-free state at 1273 K to an operating temperature of 1073 K for: (a) the cell, (b) the cell-to-foil filler metal, (c) the sealing foil, (d) the foil-to-frame filler metal, and (e) the window frame.

Please cite this article as: Weil KS, Koeppel BJ. Thermal stress analysis of the planar SOFC bonded compliant seal design. Int J Hydrogen Energy (2007), doi:10.1016/j.ijhydene.2007.11.008

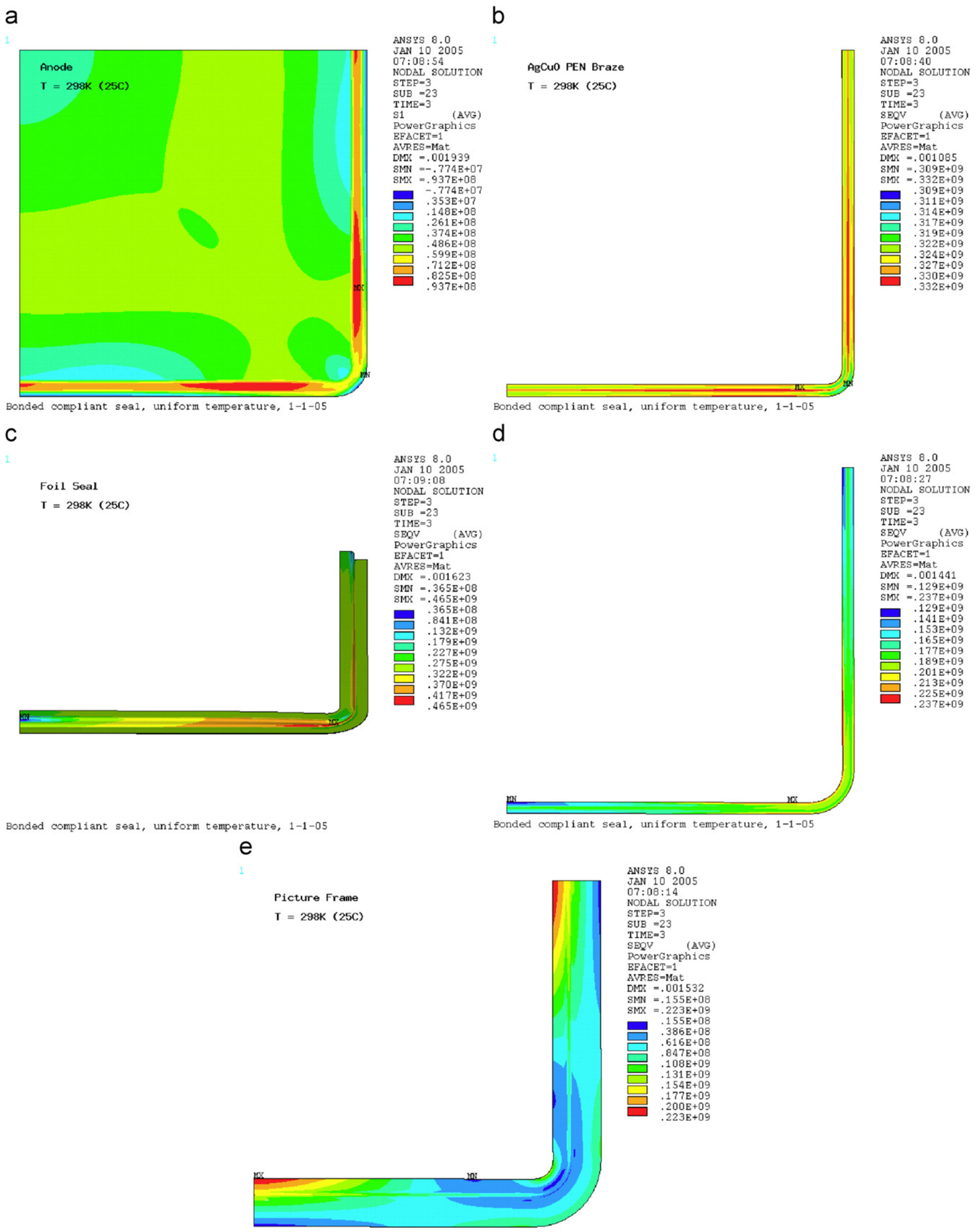

Fig. 7 – Stresses predicting upon cooling from a stress-free state at 1273 K to room temperature (298 K) for: (a) the cell, (b) the cell-to-foil filler metal, (c) the sealing foil, (d) the foil-to-frame filler metal, and (e) the window frame. The values corresponding to the scale bars listed on the right-hand side of each figure have units of Pa.

Please cite this article as: Weil KS, Koeppel BJ. Thermal stress analysis of the planar SOFC bonded compliant seal design. Int J Hydrogen Energy (2007), doi:10.1016/j.ijhydene.2007.11.008

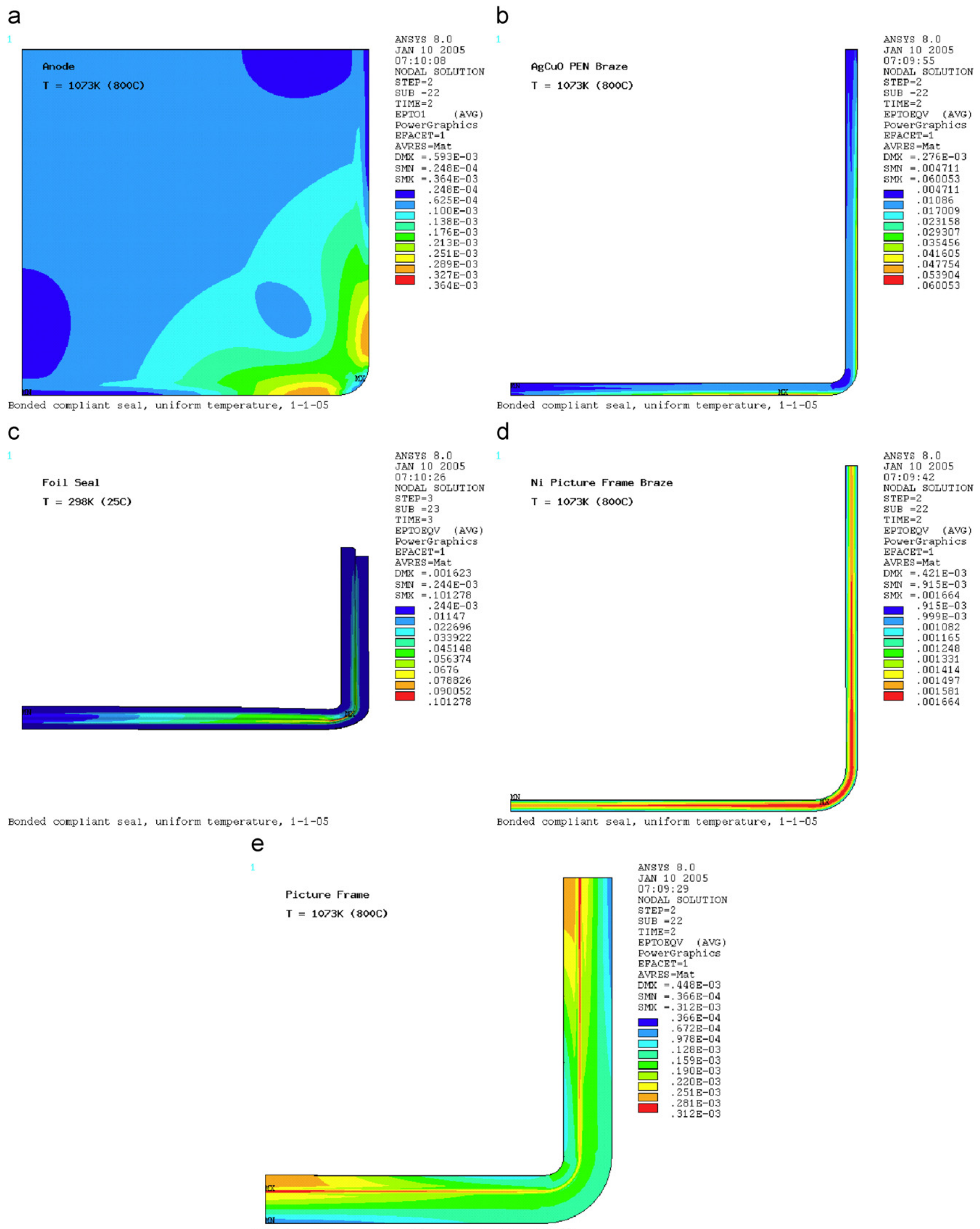

Fig. 8 – Strains predicting upon cooling from a stress-free state at 1273 K to room temperature (298 K) for: (a) the cell, (b) the cell-to-foil filler metal, (c) the sealing foil, (d) the foil-to-frame filler metal, and (e) the window frame.

Please cite this article as: Weil KS, Koeppel BJ. Thermal stress analysis of the planar SOFC bonded compliant seal design. Int J Hydrogen Energy (2007), doi:10.1016/j.ijhydene.2007.11.008

Table 2 – Maximum stresses and strains generated in each component upon cooling to 1073 and 298 K

Component	T = 1073 K		T = 298 K	
	Stress (MPa)	Strain	Stress (MPa)	Strain
Cell	22.9	0.0004	93.7	0.0010
Cell-to-foil braze	4.0	0.0601	332.0	0.0909
Sealing foil	86.5	0.0505	465.0	0.1013
Foil-to-frame braze	160.0	0.0017	237.0	0.0018
Window frame	49.4	0.0003	223.0	0.0010

that is, respectively, either 10% larger or 10% smaller in thickness. Comparison with the values in Tables 2 and 3 indicates that an increase in foil thickness tends to raise the level of maximum stress by 1.5–2.5% in the window frame and 5–10% in the cell, depending on the temperature of interest. The primary reason for this appears to be that the thicker seal is stiffer resulting in smaller deformations and a corresponding reduction in stress and strain within the sealing foil. Conversely, a reduction in foil thickness by 10% lowers the stresses in both components by as much as 10% due to greater compliance and an increase in the portion of thermal mismatch strain carried by the sealing foil. Note that neither of the two braze filler metal layers is significantly affected. That is, the difference in mechanical response caused by this simple parametric change is due to a correlation that ties the cell and the window frame directly to the foil. While further decreases in foil thickness are anticipated to lead to continued reductions in cell and window frame stresses, a limit is imposed by the oxidation resistance of the foil material and concomitant amount of metal loss expected over the lifetime of the seal.

3.2. *Part deflection as a function of temperature*

As mentioned previously, the stress-free state for the structure occurs at the brazing temperature and when cooled, thermal stresses generated in each component cause the sealing foil to deform both elastically and plastically, i.e. change in shape. Shown in Fig. 11 are a series of cross-sectional images of the seal based on the results of FE calculations conducted for the corner section. The dotted lines shown in each image indicate the original size, shape, and position of the various components in the seal. Two points are immediately apparent in this figure: (1) the cell undergoes bending (or in 3-D, bowing) and (2) in cross section, the foil assumes a more exaggerated "S" shape and eventually contacts the window frame.

Fig. 12(a) shows that out-of-plane deformation is maximum in the center of the cell, which in this model is assumed to be unsupported by any adjacent interconnect structure, leading to 2.41 mm of deflection along the 85 mm diagonal from corner to center at room temperature. A prior analysis of a barium aluminosilicate seal showed that under the same thermal conditions and using the same cell/window frame materials and geometries, cell deflection is larger in magnitude (3.61 mm at room temperature) and assumes a more complex mode [8]. Shown in Figs. 12(a)–(d) are planar and cross-sectional comparisons of cell deflection predicted when each seal design is cooled to room temperature. As seen from the diagonal cross-sectional images in Figs. 12(b) and (d), the cell undergoes simple cupping in the BCS design, whereas the cell deformation exhibits regions of different curvature when using a glass–ceramic seal. While bowing of the cell is generally not desired, some amount of simple bowing can be accommodated in stack design. However, it is anticipated that multi-modal forms of cell warpage of the type seen in Figs. 12(c) and (d) are likely to cause gas flow maldistribution, problems with electrical contact, and deleterious stresses within the multi-layer ceramic part.

From the viewpoint of cell deflection, the full-scale BCS design appears to function reasonably well. In-plane along the x- and y-directions, the sealing foil undergoes elastoplastic deformation without buckling. Out-of-plane in the z-direction, the foil collapses elastically to accommodate much of the thermal expansion mismatch between the cell and separator, although geometric non-uniformities (i.e. the corners) account for a significant amount of bowing predicted in the cell. In addition, the contact that occurs between the lower half of the foil and the window frame at some intermediate temperature above 298 K likely leads to some of the stress concentration previously identified in the cell. Thus, additional design modifications are required to mitigate the amount of cell deflection without significantly raising the state of stress in the various BCS components, particularly the cell.

The amount of allowable bowing depends on specific features of the stack which have not been included in this simplified model, e.g., allowable tolerances in the fuel flow cavity, the type/stiffness of interconnect being used, etc. In addition, the stiffness of the cell strongly impacts the amount of bowing/flexing to which the cell can be subjected and this in turn can be tailored to some degree by changing the Ni/YSZ ratio in the anode and the thicknesses of the constituent layers and by adding inert fillers such as Al_2O_3 [20,21]. Additional limitations of the current model include ignoring potential creep effects and assuming a completely uniform temperature distribution. It is expected that creep will tend to reduce stresses in the thinnest and least refractory components: the sealing foil, the cell-to-foil filler metal, and to some extent the nickel-based anode. In this regard the above model likely overestimates the maximum stresses in these components. Accurately predicting the temperature distribution

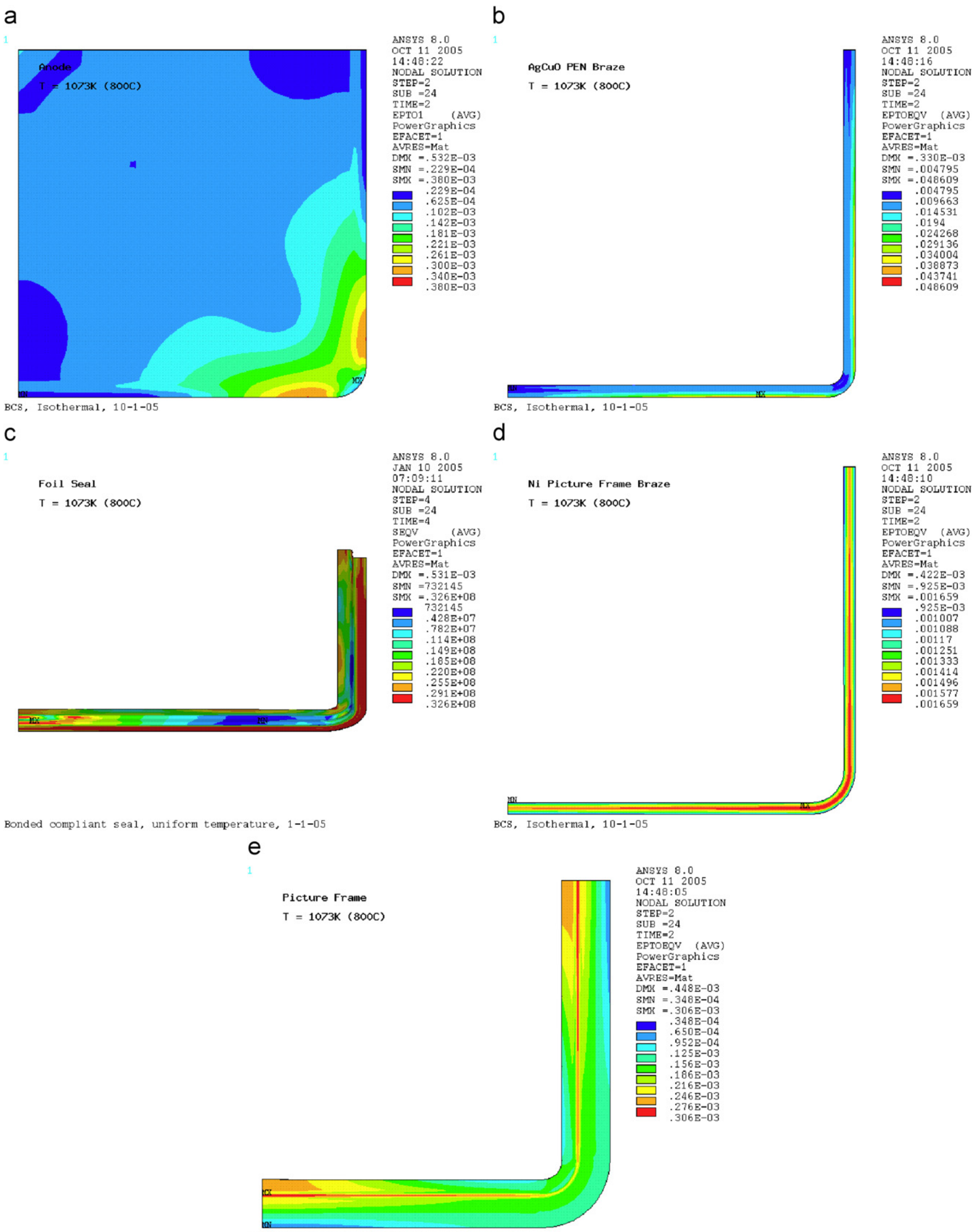

Fig. 9 – Stresses predicting upon re-heating the BCS structure to 1073 K from room temperature (298 K) for: (a) the cell, (b) the cell-to-foil filler metal, (c) the sealing foil, (d) the foil-to-frame filler metal, and (e) the window frame. Note that the values corresponding to the scale bars listed on the right-hand side of each figure have units of Pa.

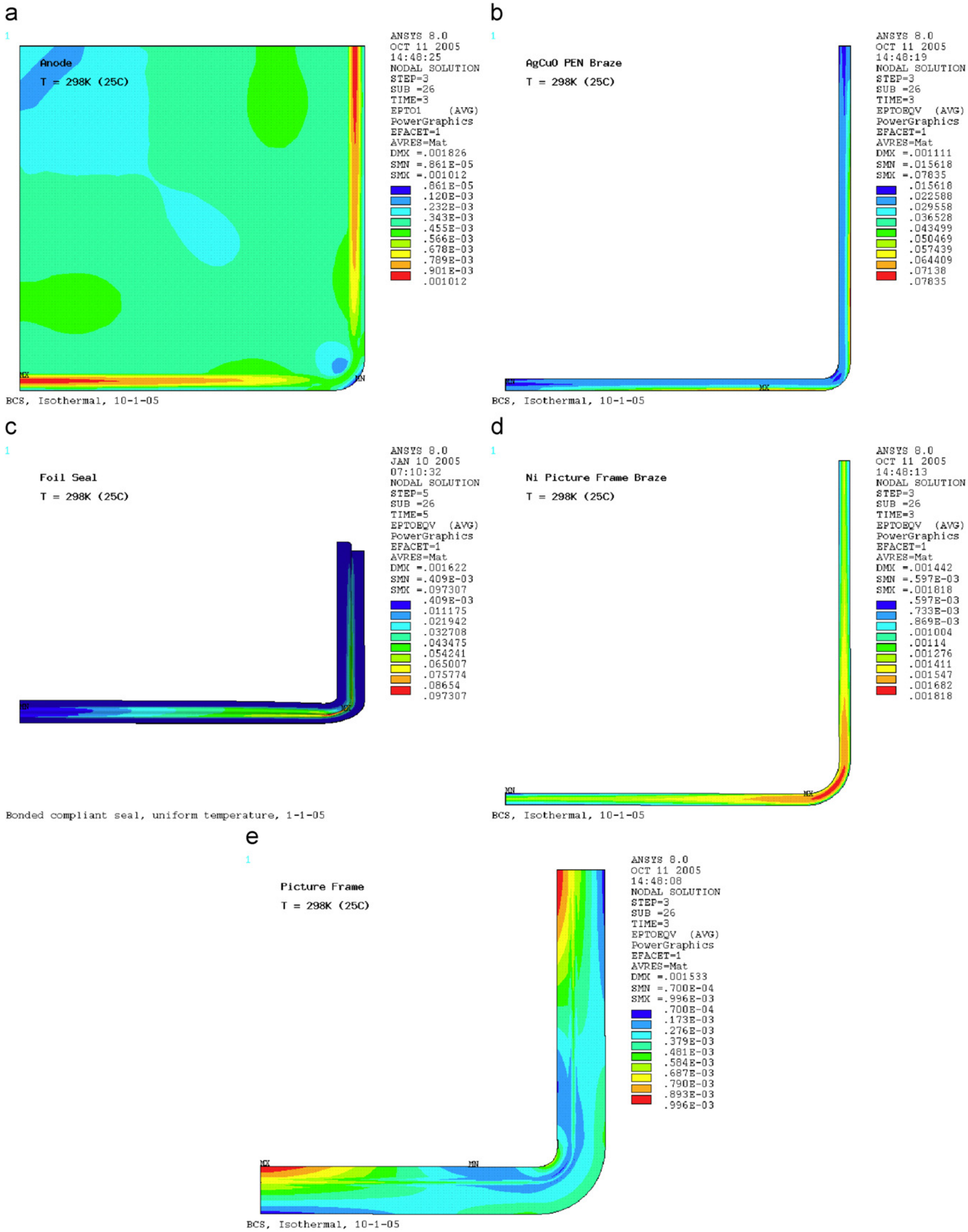

Fig. 10 – Stresses predicting upon cooling the BCS structure to room temperature (298 K) from 1073 K in a second thermal cycle for: (a) the cell, (b) the cell-to-foil filler metal, (c) the sealing foil, (d) the foil-to-frame filler metal, and (e) the window frame. Note that the values corresponding to the scale bars listed on the right-hand side of each figure have units of Pa.

Please cite this article as: Weil KS, Koeppel BJ. Thermal stress analysis of the planar SOFC bonded compliant seal design. Int J Hydrogen Energy (2007), doi:10.1016/j.ijhydene.2007.11.008

within the stack and across the various stack components can be quite complex, even under steady-state conditions. A more refined analysis will eventually include the effects of heat generation due to the electrochemical reaction, enthalpy changes due to steam reformation, and the heat removal effects of water generation across the anode among other considerations. Over the past few years, pSOFC models of increasing sophistication have been reported [22–24] and a next generation BCS design analysis that incorporates one of these can begin to account for the effects of non-uniform temperature distribution on thermal mismatch stresses/strains.

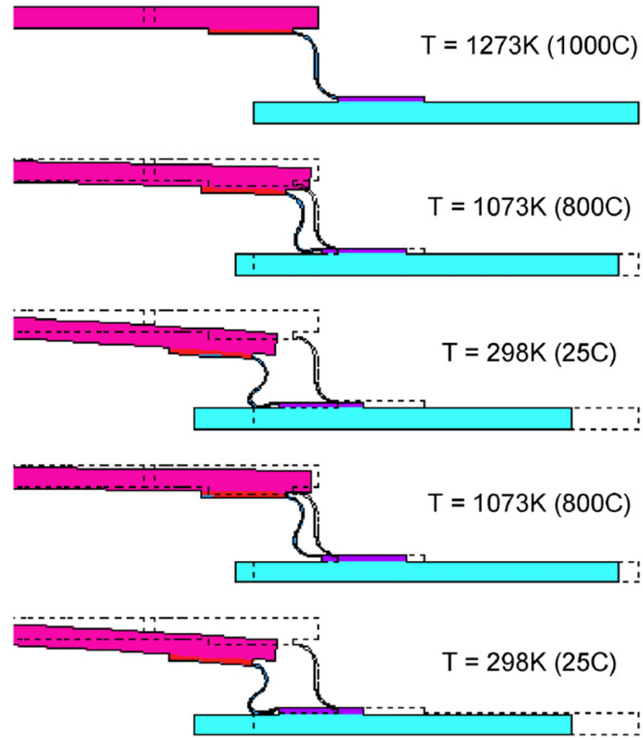

Fig. 11 – A series of cross-sectional images based from FE analysis depicting how the BCS components change in size and shape at the corner of the seal as a function of cooling from the stress-free state at 1273 K to room temperature and upon re-heating to 1073 K and cooling back to room temperature. The original size/shape of the components at the stress-free state are denoted by the dotted lines.

Table 3 – Maximum stresses and strains generated in each component upon an additional thermal cycle from room temperature to 1073 K, then back down to 298 K

Component	T = 1073 K		T = 298 K	
	Stress (MPa)	Strain	Stress (MPa)	Strain
Cell	9.2	0.0001	94.1	0.0010
Cell-to-foil braze	3.2	0.0696	333.0	0.0911
Sealing foil	32.6	0.0406	461.0	0.0973
Foil-to-frame braze	158.0	0.0018	236.0	0.0018
Window frame	30.9	0.0002	221.0	0.0010

Table 4 – Maximum thermally induced stresses and strains in a BCS design that employs a 55 μm thick sealing foil

Component					Additional thermal cycle			
	T = 1073 K		T = 298 K		T = 1073 K		T = 298 K	
	Stress (MPa)	Strain	Stress (MPa)	Strain	Stress (MPa)	Strain	Stress (MPa)	Strain
Cell	22.6	0.0004	98.7	0.0011	10.2	0.0002	98.5	0.0010
Cell-to-foil braze	4.3	0.0664	334.0	0.0978	3.4	0.0735	334.0	0.0972
Sealing foil	85.7	0.0491	456.0	0.1009	33.9	0.0408	452.0	0.0961
Foil-to-frame braze	160.0	0.0017	241.0	0.0018	158.0	0.0018	240.0	0.0018
Window frame	51.0	0.0003	241.0	0.0011	30.4	0.0002	238.0	0.0011

Table 5 – Maximum thermally induced stresses and strains in a BCS design that employs a 45 μm thick sealing foil

Component					Additional thermal cycle			
	T = 1073 K		T = 298 K		T = 1073 K		T = 298 K	
	Stress (MPa)	Strain	Stress (MPa)	Strain	Stress (MPa)	Strain	Stress (MPa)	Strain
Cell	22.8	0.0004	91.5	0.0010	8.2	0.0001	91.0	0.0010
Cell-to-foil braze	3.7	0.0533	333.0	0.0841	3.0	0.0662	333.0	0.0844
Sealing foil	87.0	0.0516	471.0	0.1027	32.7	0.0410	463.0	0.0994
Foil-to-frame braze	160.0	0.0017	233.0	0.0018	158.0	0.0018	232.0	0.0018
Window frame	47.7	0.0003	205.0	0.0009	31.5	0.0002	203.0	0.0009

Please cite this article as: Weil KS, Koeppel BJ. Thermal stress analysis of the planar SOFC bonded compliant seal design. Int J Hydrogen Energy (2007), doi:10.1016/j.ijhydene.2007.11.008

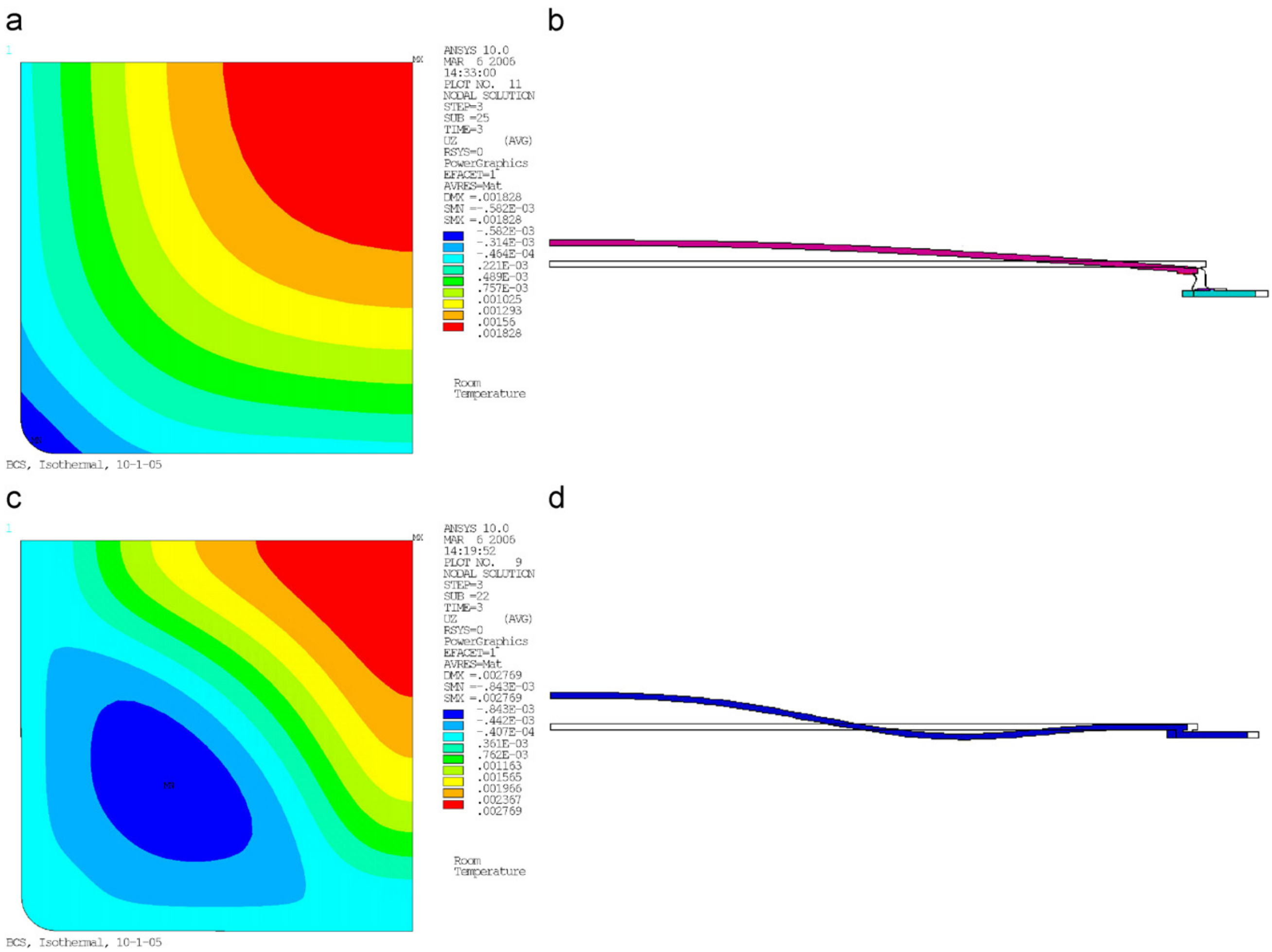

Fig. 12 – Schematics of cell deflection for the BCS seal design: (a) contours of out-of-plane deformation in the quarter-symmetry model and (b) cross-sectional view along the diagonal of the cell. Schematics of cell deflection for a barium aluminosilicate glass–ceramic seal design seal design: (c) contours of out-of-plane deformation in the quarter-symmetry model, and (d) cross-sectional view along the diagonal of the cell [8]. Note in (a) and (c) that the values corresponding to the gray-scale bars listed on the bottom of each have units of meters and in (b) and (d) the original size/shape of the components at the stress-free state are denoted by the black and white lines.

4. Conclusions

FE analysis was used to investigate the effects of scaling and geometry on the thermal cycling performance of a BCS design that employed a window frame material with approximately a 50% CTE mismatch with a typical anode-supported pSOFC cell. In general the initial seal design is predicted to work well in terms of thermal stress reduction, but will likely require further modification to reduce the potential for excessive cell bowing. The amount of bowing is relatively small when the structure is cooled to the operating temperature (800 °C), but increases up to ~2.4 mm (as measured from the corner of the cell to its center) when cooled completely down to room temperature. However, the thermal stresses that develop within the structure at these temperatures are effectively transferred to the sealing foil and soft silver-based cell-to-foil braze layer, where they are absorbed as elastic and plastic strain. The maximum stresses and strains calculated in each component during each thermal cycle are within acceptable limits for each of the materials under consideration. When the structure is computationally subjected to a second thermal cycle, nearly all of the component stresses are found to be lower than those experienced in the first cycle.

The current design is slightly flawed in that the foil dimensions are such that when cooled to room temperature the foil makes contact with the window frame, which likely leads to higher stresses in the cell, seal, and frame. It is anticipated that this can be easily rectified with a minor change in the thickness or cross-sectional shape of the sealing foil. For example, an initial analysis of the effect of foil thickness on component stresses and strains indicated that by decreasing foil gage 10%, a 5–15% reduction in maximum stress/strain could be achieved. However, more work is needed to understand the effects of the BCS design variables on the stresses and strains that arise in the components, particularly foil stiffness and geometry. In addition, next generation designs should account for non-uniform temperature distributions that arise across the cell

Please cite this article as: Weil KS, Koeppel BJ. Thermal stress analysis of the planar SOFC bonded compliant seal design. Int J Hydrogen Energy (2007), doi:10.1016/j.ijhydene.2007.11.008

due to gas manifold design and placement and to electrochemical and reforming reactions that occur within the stack.

Acknowledgments

This work was supported by the US Department of Energy as part of the SECA Program. The Pacific Northwest National Laboratory is operated by Battelle Memorial Institute for the United States Department of Energy (US DOE) under Contract DE-AC06-76RLO 1830.

REFERENCES

[1] Iwata T, Enami Y. J Electrochem Soc 1998;145:931.
[2] Hartvigsen J, Milliken J, Elangovan S, Khandkar A. In: Ceramic Transactions, vol. 65. Westerville, OH: American Ceramic Society; 1996 p.279.
[3] Fergus J. J Power Sources 2005;147:46.
[4] Weil KS. JOM 2006;58:37.
[5] Yang Z, Weil KS, Paxton DM, Stevenson JW. J Electrochem Soc 2003;150:A1188.
[6] Hilpert K, Das D, Miller M, Peck DH, Weiss R. J Electrochem Soc 1996;143:3642.
[7] Weil KS, Hardy JS, Koeppel BJ. J Mater Eng Perform 2006;15:427.
[8] K.S. Weil, B.J. Koeppel, J Power Sources, in review.
[9] Weil KS, Kim JY, Hardy JS. Electrochem Solid State Lett 2005;8:A133.
[10] S. Mukerjee, S. Shaffer, J. Zizelman, L. Chick, S. Baskaran, C. Coyle, et al., *Eighth international symposium solid oxide fuel cells*, vol. 2003, The Electrochemical Society, 2003.
[11] N.Q. Minh, P. Kelly, K. Montgomery, *Second european solid oxide fuel cell forum. Proceedings*, vol. 2 (Part 2), 1996. p. 659.
[12] Haynes international (www.haynesintl.com).
[13] Engineered materials solutions (www.emsclad.com).
[14] Metals handbook, 9th ed. vols. 2, 3. American Society for Metals, 1980.
[15] Personal communication, J.P. Keaveney, Pacific Northwest National Laboratory.
[16] Baran NM. Finite element analysis on microcomputers. New York: McGraw-Hill Book Company; 1988.
[17] Lin C-K, Chen T-T, Chyou Y-P, Chiang L-K. J Power Sources 2007;164:238.
[18] Kotlowitz RW. IEEE Trans Components Hybrids Manuf Technol 1989;12:431.
[19] Rigal E, Bucci P, Le Marois G. Fusion Eng Des 2000;49-50: 317.
[20] Svoboda RJ, Simpkins H, Keller J, Sprenkle VL, Meinhardt KD, Canfield NL. US Patent 20050202159, issued 09/15/2005.
[21] Malzbender J, Wakai T, Steinbrech RW. Fuel Cells 2006;6:123.
[22] Recknagle KP, Williford RE, Chick LA, Rector DR, Khaleel MA. J Power Sources 2003;113:109.
[23] Campanari S, Iora P. Fuel Cells 2005;5:34.
[24] Yang Y, Wang G, Zhang H, Xia W. J Power Sources 2007;167: 398.

Please cite this article as: Weil KS, Koeppel BJ. Thermal stress analysis of the planar SOFC bonded compliant seal design. Int J Hydrogen Energy (2007), doi:10.1016/j.ijhydene.2007.11.008